Catal Lett (2008) 121:209–218
DOI 10.1007/s10562-007-9369-1

Novel $Au/TiO_2/Al_2O_3 \cdot xH_2O$ catalysts for CO oxidation

Wen Fu Yan · Zhen Ma · Shannon M. Mahurin · Jian Jiao · Edward W. Hagaman · Steven H. Overbury · Sheng Dai

Received: 6 November 2007 / Accepted: 17 November 2007 / Published online: 12 December 2007

Abstract $Au/Al_2O_3 \cdot xH_2O$ and $Au/TiO_2/Al_2O_3 \cdot xH_2O$ ($x = 0$–3) catalysts were prepared by assembling gold nanoparticles on neat and TiO_2-modified Al_2O_3, AlOOH, and $Al(OH)_3$ supports, and their catalytic activity in CO oxidation was tested either as synthesized or after on-line pretreatment in O_2–He at 500 °C. A promotional effect of TiO_2 on the activity of gold catalysts was observed upon 500 °C-pretreatment. The catalyst stability as a function of time on stream was tested in the absence or presence of H_2, and physiochemical characterization applying BET, ICP-OES, XRD, TEM, and ^{27}Al MAS NMR was conducted.

Keywords Gold catalysts · Nanoparticles · TiO_2 · Al_2O_3 · CO oxidation · Activity · Promotion

1 Introduction

Heterogeneous gold catalysis has attracted much attention recently, as supported gold nanoparticles have many applications in environmental control, chemical synthesis, and energy conversion [1–5]. TiO_2 is a reducible support that can activate O_2 for CO oxidation [6], and it is frequently used for preparing supported gold catalysts [1–5]. Nevertheless, the activity of Au/TiO_2 decreases significantly upon thermal treatment above 400 °C due to the agglomeration of gold nanoparticles [7–10]. On the other hand, the activity of Au/Al_2O_3 in CO oxidation is generally lower than that of Au/TiO_2 [6], and Au/Al_2O_3 is less frequently studied [11–18]. So far, limited attempts have been made to promote Au/Al_2O_3 by putting additives [19–24], and virtually no work has systematically used $Al_2O_3 \cdot xH_2O$ ($x = 0$–3: aluminium oxide, oxyhydroxide, and hydroxide) supports other than γ-Al_2O_3 for loading gold [4].

We are interested in the development of novel gold catalysts via modification of the surface of the support [10, 25–32]. We previously showed that the modification of TiO_2 supports by amorphous Al_2O_3 additive could stabilize gold nanoparticles against sintering [10, 29]. In the current letter, we employed a surface-sol–gel method to modify a series of $Al_2O_3 \cdot xH_2O$ ($x = 0$–3) supports with TiO_2 additive, followed by assembling gold nanoparticles. It was found that some $Au/TiO_2/Al_2O_3 \cdot xH_2O$ catalysts, after pretreatment at 500 °C, could achieve higher activity in CO oxidation than $Au/Al_2O_3 \cdot xH_2O$, $Au/Al_2O_3/TiO_2$ [10, 29], and a reference Au/TiO_2 catalyst furnished by World Gould Council. The catalyst stability as a function of reaction time was tested, and relevant characterization by BET, ICP-OES, XRD, TEM, and ^{27}Al MAS NMR was conducted.

2 Experimental

Boehmite AlOOH (nanoparticle whiskers, Aldrich, CAT#: 551643-10G), boehmite AlOOH (CATAPAL A, Sasol North America Inc., LOT#: P13091), amorphous $Al(OH)_3$ (Aldrich), and highly-crystalline γ-Al_2O_3 (Aldrich, CAT#: 544833-50G) were used as supports or support precursors.

W. F. Yan · Z. Ma · S. M. Mahurin · J. Jiao · E. W. Hagaman · S. H. Overbury · S. Dai (✉)
Chemical Sciences Division, Oak Ridge National Laboratory, Oak Ridge, TN 37831, USA
e-mail: dais@ornl.gov

W. F. Yan
State Key Laboratory of Inorganic Synthesis and Preparative Chemistry, College of Chemistry, Jilin University, Changchun 130012, P.R. China

To prepared nanosized γ-Al_2O_3, AlOOH (Aldrich or CATAPAL A) was calcined in a muffle oven at 500 °C under static air for 2 h. The identities of these materials were checked by XRD.

$TiO_2/Al_2O_3 \cdot xH_2O$ supports were prepared by a surface-sol–gel method [27, 33]. About 3.0 g $Al_2O_3 \cdot xH_2O$ and a stirring bar were loaded in a reflux bottle and dried at 125 °C for 16 h. The reflux bottle was sealed by a predried rubber septum, and 4.0 mL $Ti(OC_4H_9)_4$, 20 mL anhydrous toluene, and 20 mL anhydrous methanol transferred into the bottle through a syringe, and the solution refluxed for 3 h. The product was filtered, washed several times with absolute ethanol and deionized water, and dried at 80 °C overnight.

Gold was loaded onto $Al_2O_3 \cdot xH_2O$ or $TiO_2/Al_2O_3 \cdot xH_2O$ supports via a deposition–precipitation method [1–5]. Fifty milliliter of aqueous solution containing 0.3 g $HAuCl_4 \cdot 3H_2O$ was titrated by 1.0 M KOH to pH 10.0, and heated at 80 °C followed by adding 1.0 g support. The mixture was stirred for 2 h. The precipitates were separated by centrifugation and washed three times with deionized water and once with ethanol. The product was dried at 40 °C to obtain the as-synthesized catalyst.

CO oxidation was tested in an Altamira AMI 200 plug-flow microreactor. For activity measurements, 50 mg catalyst was loaded into a U-shaped quartz tube (4 mm i.d.), but for stability tests less sample was used to avoid seeing 100% conversion all the time [4]. The catalyst was either tested as synthesized or pretreated in the reactor in flowing 8% O_2 (balance He) at 500 °C for 2.5 h. After the pretreatment, the catalyst was cooled down, the gas stream switched to 1% CO (balance air) and the reaction temperature ramped using a furnace or by immersing the U-shaped tube in ice-water or acetone–liquid nitrogen. The flow rate of reactant stream was 37 cm^3/min. A portion of the product was extracted periodically with an automatic sampling valve, and analyzed using a dual-column gas chromatograph with a thermal conductivity detector. The CO conversion was calculated as $X_{CO} = [CO_2]_{out}/([CO]_{out} + [CO_2]_{out})$. Proper calibration was conducted to determine the correction factors of CO and CO_2 peak areas.

BET surface areas were measured by N_2 adsorption–desorption at 77 K using a Micromeritics Gemini instrument. The Au and Ti contents were analyzed by inductivity coupled plasma-optical emission spectrometry (ICP-OES) on a Thermo IRIS Intrepid II spectrometer. XRD data were collected on a Siemens D5005 diffractometer with CuK_α radiation. TEM experiments were carried out on a Hitachi HD-2000 STEM instrument operated at 200 kV. ^{27}Al MAS NMR experiments were carried out on a Bruker AVANCE 400 ($B_0 = 9.4$ T) spectrometer at a resonance frequency of 104.2 MHz spinning up to 14 kHz. ^{27}Al 3QMAS NMR spectra were obtained by applying z-filter 3QMAS pulse sequence [34] with $p_1 = 4.0$ μs, $p_2 = 1.4$ μs, $p_3 = 40$ μs and recycle delay of 1.0 s. Chemical shifts were referenced to 1.0 M $Al(NO_3)_3$: $\delta = 0$ ppm. The isotropic chemical shift (δ_{CS}) and second order quadrupolar effect (SOQE) were calculated from δ_{F1} and δ_{F2} in the 3QMAS NMR spectrum [35].

3 Results

3.1 Au/AlOOH and Au/γ-Al_2O_3

AlOOH (Aldrich) and AlOOH (CATAPAL A) supports exhibited typical XRD patterns of nanocrystalline boehmite. They both transformed into nanocrystalline γ-Al_2O_3 upon calcination in a muffle oven at 500 °C (data not shown). These four supports were then used to load gold in the initial phase of our research. The supported gold catalysts were tested either as synthesized or after on-line pretreatment in O_2–He at 500 °C prior to the reaction testing. The Al_2O_3 phase in as-synthesized and 500 °C-pretreated Au/γ-Al_2O_3 samples was determined by XRD as γ-Al_2O_3, but the boehmite phase of as-synthesized Au/AlOOH transformed into γ-Al_2O_3 phase upon pretreatment in the reactor at 500 °C (data not shown).

Figure 1a shows the conversion curves of Au/γ-Al_2O_3. This γ-Al_2O_3 support was derived from calcining AlOOH (CATAPAL A) in a muffle oven at 500 °C. As-synthesized Au/γ-Al_2O_3 showed a T_{50} (temperature required for 50% conversion) value of −8 °C. After pretreating this catalyst at 500 °C, the conversion curve shifted to higher temperatures, and the T_{50} value increased to 17 °C. Additional experiments indicated that the T_{50} values of four as-synthesized Au/AlOOH and Au/γ-Al_2O_3 samples were in the range of −31 and −8 °C, whereas those of 500 °C-pretreated samples were in the range of −21 and 36 °C (Table 1). Such loss in activity is less severe than that observed on Au/TiO_2, where the T_{50} value increased from −55 to 125 °C upon 500 °C-pretreatment [10].

Z-contrast TEM images of as-synthesized and 500 °C-pretreated Au/γ-Al_2O_3 are shown in Fig. 2a and b. As-synthesized Au/γ-Al_2O_3 exhibited tiny gold clusters (0.5–1 nm, white dots) barely visible (Fig. 2a). After 500 °C-pretreatment and subsequent reaction testing, gold clusters on γ-Al_2O_3 evolved to bigger particles with sizes of 2–4 nm (Fig. 2b). Gold nanoparticles with these sizes are known to be active for CO oxidation [1–5]. However, in our previous publication, after pretreating Au/TiO_2 at 500 °C, gold particle sizes were in the range of 5–30 nm [10]. Therefore, it appears that γ-Al_2O_3 is different from TiO_2 support in terms of the thermal stability of supported gold nanoparticles. Further theoretical work concerning the difference is worthwhile in the future.

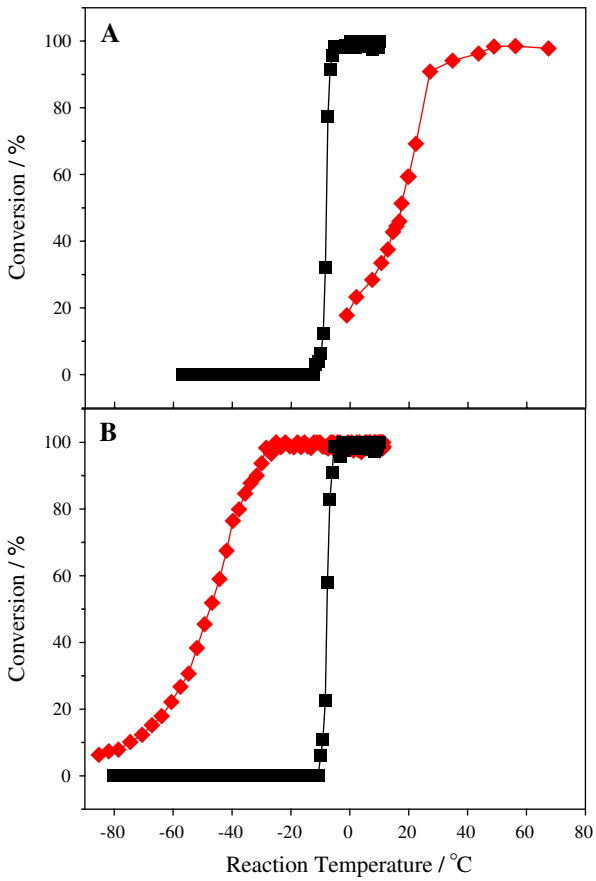

Fig. 1 (**a**) Conversion curves of as-synthesized (■) and 500 °C-pretreated (◆) $Au/\gamma\text{-}Al_2O_3$. (**b**) Conversion curves of as-synthesized (■) and 500 °C-pretreated (◆) $Au/TiO_2/\gamma\text{-}Al_2O_3$. The $\gamma\text{-}Al_2O_3$ was from calcining AlOOH (CATAPAL) in a muffle oven at 500 °C

3.2 $Au/TiO_2/AlOOH$ and $Au/TiO_2/\gamma\text{-}Al_2O_3$

Four AlOOH and $\gamma\text{-}Al_2O_3$ supports mentioned in Sect. 3.1 were then modified by TiO_2. No crystalline TiO_2 was detected by XRD, indicating the amorphous nature of the TiO_2 decoration (data not shown). The TiO_2/AlOOH and $TiO_2/\gamma\text{-}Al_2O_3$ supports were not subject to elemental analysis, but the presence of Ti element in Au/TiO_2/AlOOH and $Au/TiO_2/\gamma\text{-}Al_2O_3$ catalysts was verified and quantitatively measured by ICP-OES (Table 1). Although the Ti(IV) species from surface-sol–gel processing of titanium(IV) alkoxide has uncondensed hydroxyl groups, it is often denoted as TiO_2 for convenience [25, 26, 33, 36–39]. After loading gold, these four catalysts were tested either as synthesized or after pretreatment in O_2–He at 500 °C. The Al_2O_3 phases in as-synthesized and 500 °C-pretreated $Au/TiO_2/\gamma\text{-}Al_2O_3$ samples was $\gamma\text{-}Al_2O_3$, but the boehmite phase of as-synthesized Au/TiO_2/AlOOH transformed to $\gamma\text{-}Al_2O_3$ phase after pretreatment at 500 °C (data not shown). As shown in Table 1, the Ti contents of the TiO_2-containing catalysts were in the range of 1.6 and 2.2 wt.%, and the introduction of TiO_2 did not significantly perturb the gold loading (e.g., 5.7 and 5.2 wt.%, for Au/AlOOH-Aldrich and Au/TiO_2/AlOOH-Aldrich, respectively).

Figure 1b shows the conversion curves of $Au/TiO_2/\gamma\text{-}Al_2O_3$. This $\gamma\text{-}Al_2O_3$ was prepared by calcining AlOOH (CATAPAL A) in a muffle oven at 500 °C. As-synthesized $Au/TiO_2/\gamma\text{-}Al_2O_3$ exhibited a T_{50} value of −8 °C (Fig. 1b), the same as as-synthesized $Au/\gamma\text{-}Al_2O_3$ (Fig. 1a). Interestingly, after pretreating this catalyst at 500 °C, the conversion curve shifted to lower temperatures, and the T_{50} value decreased to −48 °C. This pretreatment-induced activity increase was observed in other systems (Table 1). For instance, the T_{50} value of as-synthesized $Au/TiO_2/\gamma\text{-}Al_2O_3$ ($\gamma\text{-}Al_2O_3$ in this case was prepared by calcining AlOOH-Aldrich at 500 °C) was −20 °C, but that of 500 °C-pretreated catalyst was −46 °C (Fig. 3). This is different from the published case of $Au/Al_2O_3/TiO_2$, in

Table 1 BET surface areas of the supports, the elemental analysis data of the as-synthesized catalysts, and the T_{50} values of as-synthesized and 500 °C-pretreated catalysts

Support		Catalyst			
Type	Surface area/m^2/g	Ti loading/wt.%	Au loading/wt.%	T_{50} (as-synthesized)/°C	T_{50} (500 °C-pretreated)/°C
AlOOH (Aldrich)	207	–	5.7	−20	14
TiO_2/AlOOH (Aldrich)	–	1.6	5.2	−14	−48
$\gamma\text{-}Al_2O_3$ from calcining AlOOH (Aldrich)	180	–	7.2	−31	−21
$TiO_2/\gamma\text{-}Al_2O_3$ from calcining AlOOH (Aldrich)	–	2.1	7.4	−20	−46
AlOOH (CATAPAL A)	260	–	7.4	−23	36
TiO_2/AlOOH (CATAPAL A)	–	1.9	7.6	−24	−20
$\gamma\text{-}Al_2O_3$ from calcining AlOOH (CATAPAL A)	230	–	3.7	−8	17
$TiO_2/\gamma\text{-}Al_2O_3$ from calcining AlOOH (CATAPAL A)	–	2.2	4.1	−8	−48

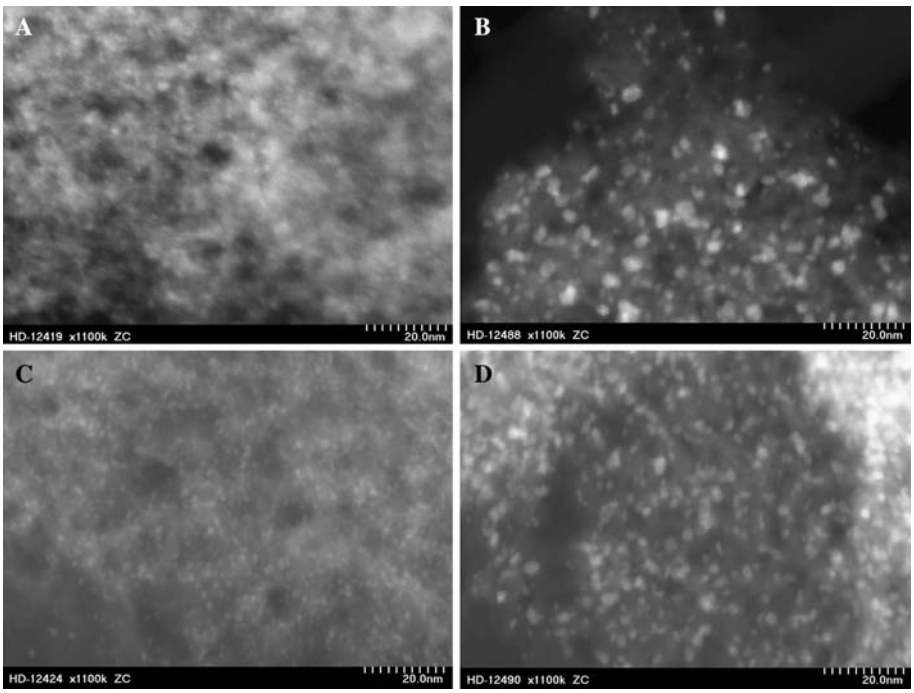

Fig. 2 Z-contrast TEM images of as-synthesized Au/γ-Al_2O_3 (**a**), 500 °C-pretreated Au/γ-Al_2O_3 (**b**), as-synthesized Au/TiO_2/γ-Al_2O_3 (**c**), and 500 °C-pretreated Au/TiO_2/γ-Al_2O_3 (**d**). The γ-Al_2O_3 was from calcining AlOOH (CATAPAL) in a muffle oven at 500 °C. The scale bar of the TEM images is 20.0 nm

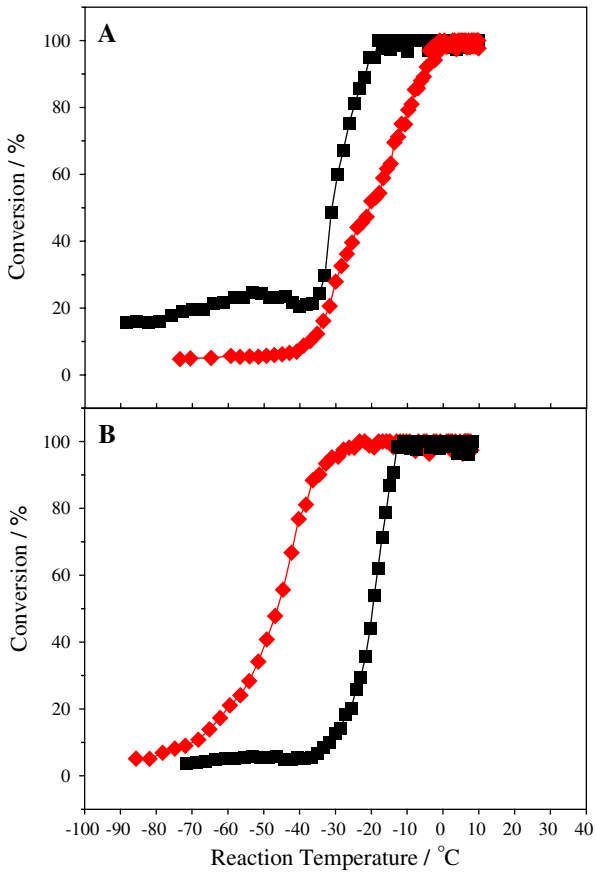

Fig. 3 (**a**) Conversion curves of as-synthesized (■) and 500 °C-pretreated (◆) Au/γ-Al_2O_3. (**b**) Conversion curves of as-synthesized (■) and 500 °C-pretreated (◆) Au/TiO_2/γ-Al_2O_3. The γ-Al_2O_3 was from calcining AlOOH (Aldrich) in a muffle oven at 500 °C

which pretreating Au/Al_2O_3/TiO_2 at 500 °C made the catalyst less active, increasing the T_{50} value from −40 to 17 °C [10].

Z-contrast TEM images of as-synthesized and 500 °C-pretreated Au/TiO_2/γ-Al_2O_3 are shown in Fig. 2c and d, respectively. As-synthesized Au/TiO_2/γ-Al_2O_3 showed gold clusters (0.5–1 nm, white dots) barely visible (Fig. 2c). After 500 °C-pretreatment and subsequent reaction testing, gold particles on TiO_2/γ-Al_2O_3 (Fig. 2d) were a little bit smaller than, or at least comparable to, those of 500 °C-pretreated Au/γ-Al_2O_3 (Fig. 2b), but that does not wholly explain the much superior activity of 500 °C-pretreated Au/TiO_2/γ-Al_2O_3 ($T_{50} = -48$ °C) compared to that of calcined Au/γ-Al_2O_3 ($T_{50} = 17$ °C). Moreover, in several examples, the activity of 500 °C-pretreated Au/TiO_2/$Al_2O_3 \cdot xH_2O$ was higher than that of 500 °C-pretreated Au/$Al_2O_3 \cdot xH_2O$ (Table 1), even though the gold particles of the former were sometimes bigger than those of the latter (Fig. 4 and other data not shown).

Au/TiO_2 (1.5 wt.% Au) furnished by World Gold Council (WGC) was tested for reference. The T_{50} values of as-synthesized and 500 °C-pretreated Au/TiO_2 (WGC) were −29 and 7 °C, respectively. The decrease in activity of Au/TiO_2 (WGC) after 500 °C-pretreatment was not as drastic as that of Au/TiO_2 (Degussa P25) prepared by us [10], due to different gold content (1.5 wt.% for WGC catalyst versus 6.7 wt.% in our previous publication [10]) and preparation details. Even though Au/TiO_2 (WGC) is highly active, our Au/TiO_2/AlOOH and Au/TiO_2/γ-Al_2O_3 catalysts exhibited even higher activity after 500 °C-pretreatment (Table 1).

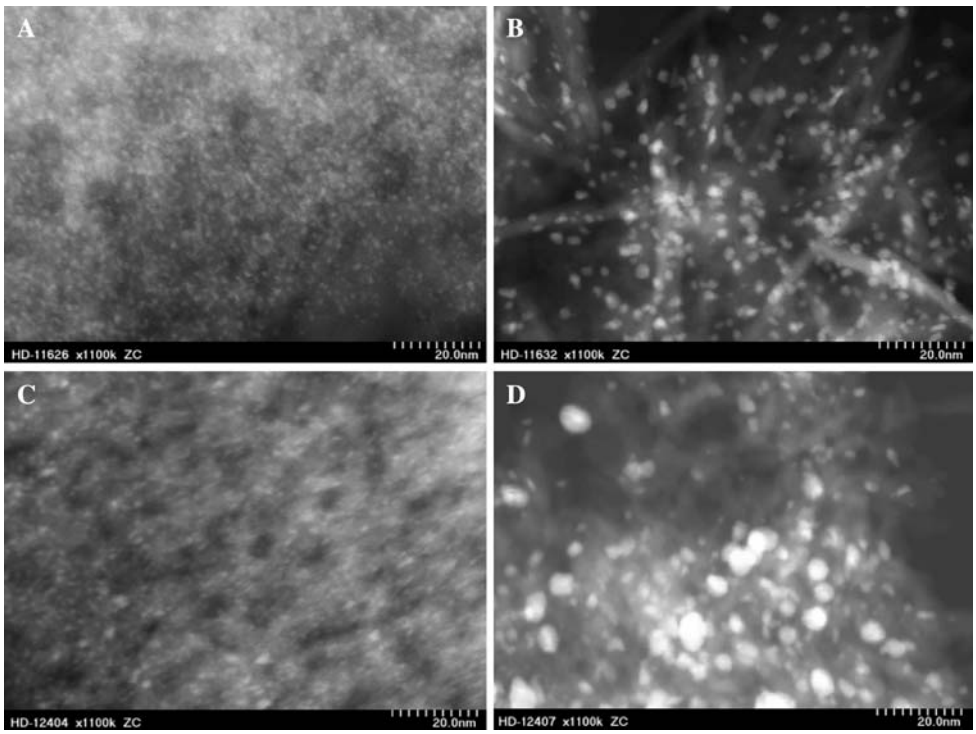

Fig. 4 Z-contrast TEM images of as-synthesized Au/γ-Al_2O_3 (**a**), 500 °C-pretreated Au/γ-Al_2O_3 (**b**), as-synthesized Au/TiO_2/γ-Al_2O_3 (**c**), and 500 °C-pretreated Au/TiO_2/γ-Al_2O_3 (**d**). The γ-Al_2O_3 was from calcining AlOOH (Aldrich) in a muffle oven at 500 °C. The scale bar of the TEM images is 20.0 nm

At the reaction temperature of −40 °C, 500 °C-pretreated Au/TiO_2/γ-Al_2O_3 (calcined AlOOH-Aldrich) showed a high specific rate of 0.21 mol g_{Au}^{-1} h^{-1}, whereas as-supplied Au/TiO_2 (WGC) showed a specific rate of 0.06 mol g_{Au}^{-1} h^{-1}.

It should be mentioned that 500 °C-pretreated Au/TiO_2/Al_2O_3 · xH_2O samples were not always more active than as-synthesized Au/TiO_2/Al_2O_3 · xH_2O. In the latter phase of our research, amorphous $Al(OH)_3$ and highly-crystalline γ-Al_2O_3 were used as supports or support precursors (Figs. 5, 6). It was found that 500 °C-pretreated Au/TiO_2/$Al(OH)_3$ was more active than 500 °C-pretreated Au/$Al(OH)_3$, but less active than as-synthesized Au/TiO_2/$Al(OH)_3$ (Fig. 5). In this case, unmodified Au/$Al(OH)_3$ lost activity more drastically after 500 °C-pretreatment (as the case with Au/amorphous Al_2O_3 previously reported by Ma et al. [29]), so even if extra TiO_2 additives promoted the activity, the overall activity after 500 °C-pretreatment was still low. This is different from the cases in Figs. 1 and 3, where 500 °C-pretreated Au/γ-Al_2O_3 was still active, so the promotional effect of TiO_2 was more obvious when it was used to promote such "superior" Au/γ-Al_2O_3.

3.3 Stability Tests and Catalyst Regeneration

We tested the stability of several catalysts, because of its importance for practical purposes [40, 41]. Less catalyst was loaded in the reactor to make sure that the conversion would not reach 100% [4, 42], considering that the regular load (50 mg) required in the light-off curve measurements would lead to 100% conversion at room temperature and bias the stability trends. As shown in Fig. 7, the deactivation of 500 °C-pretreated Au/γ-Al_2O_3 (γ-Al_2O_3 was produced from calcining AlOOH-Aldrich at 500 °C) during CO oxidation was clearly observed, consistent with the literature on the deactivation of Au/Al_2O_3 [12–14], possibly due to the accumulation of carbonate species [13]. The presence of TiO_2 in Au/TiO_2/γ-Al_2O_3 did not avoid the deactivation as shown in Fig. 7. We also tested Au/γ-Al_2O_3 (calcined CATAPAL A) and Au/TiO_2/γ-Al_2O_3 (calcined CATAPAL A), and observed similar trends (data not shown).

The deactivated catalysts could be regenerated subsequently by on-line treatment in O_2–He at 400 °C. In addition, the deactivation of Au/TiO_2/γ-Al_2O_3 seen in Fig. 7 could be suppressed in the presence of H_2 (Fig. 8). The experimental conditions are specified in the caption of Fig. 8. During that test period, around 20% of the H_2 gas was consumed. Similarly, we previously noticed that the deactivation of several gold catalysts in CO oxidation could be mitigated in the presence of H_2 [28, 29]. It was proposed in the literature that the formation of water from H_2 oxidation may clean up the surface carbonate species, thus suppressing the deactivation of gold catalysts [43, 44]. Further systematic spectroscopic experiments could be worthwhile to clarify this point.

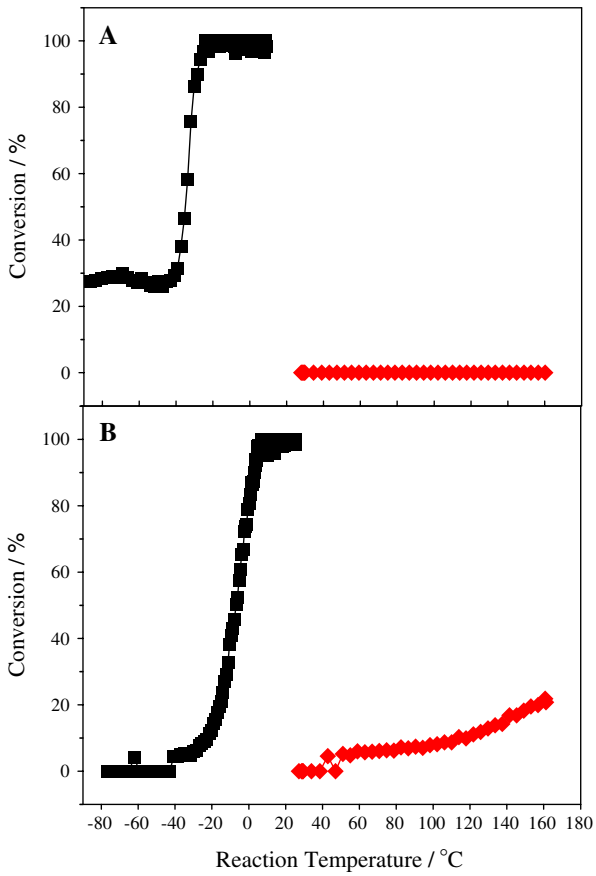

Fig. 5 (**a**) Conversion curves of as-synthesized (■) and 500 °C-pretreated (◆) $Au/Al(OH)_3$. (**b**) Conversion curves of as-synthesized (■) and 500 °C-pretreated (◆) $Au/TiO_2/Al(OH)_3$. The $Al(OH)_3$ support was an amorphous powder from Aldrich

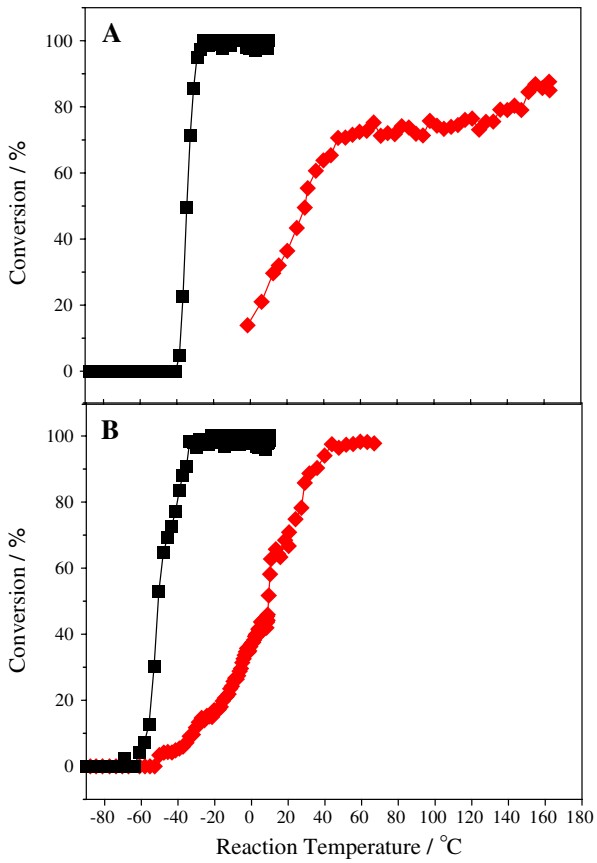

Fig. 6 (**a**) Conversion curves of as-synthesized (■) and 500 °C-pretreated (◆) $Au/\gamma\text{-}Al_2O_3$. (**b**) Conversion curves of as-synthesized (■) and 500 °C-pretreated (◆) $Au/TiO_2/\gamma\text{-}Al_2O_3$. The $\gamma\text{-}Al_2O_3$ support was a highly crystalline powder from Aldrich

3.4 NMR Studies of Catalysts

^{27}Al 3QMAS NMR experiments were performed to better understand the effects of the heat treatments upon the catalysts. Figure 9 shows the ^{27}Al 3QMAS NMR spectra of two different samples in the as-synthesized state and in the 500 °C-pretreated state. Figure 10 shows the projections of these signals along the isotropic chemical shift axis (F_2, left side) and along the quadrupole axis (F_1, right side). Three distinct signals were resolved and may be assigned to tetrahedral Al (signal **1**) and two types of octahedral Al (signal **2** and **3**) environments. Signals **1** and **3** are typical of Al in $\gamma\text{-}Al_2O_3$ [45, 46], whereas the additional octahedral site (signal **2**) is assigned to surface-related Al–OH groups [47].

In the Au/Al_2O_3 sample, 500 °C-pretreatment appears to cause a decrease in signal **2** relative to signal **3**, indicative of conversion of a portion of the octahedral Al–OH groups (signal **2**) into typical octahedral Al (signal **3**), a process that could be due to heat-induced dehydroxylation

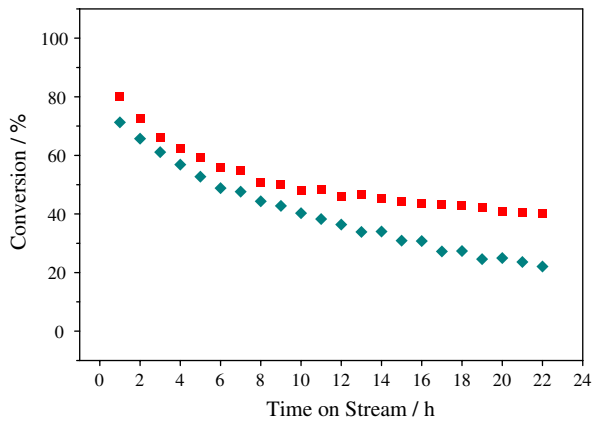

Fig. 7 Stability tests. In these experiments, 37 mL/min 1% CO (balance air) continuously flowed through 30 mg 500 °C-pretreated $Au/\gamma\text{-}Al_2O_3$ at 20 °C (■) or 12 mg 500 °C-pretreated $Au/TiO_2/\gamma\text{-}Al_2O_3$ at 23 °C (◆). The $\gamma\text{-}Al_2O_3$ was from calcining AlOOH (Aldrich) in a muffle oven at 500 °C

(Fig. 10a, b). This conversion was less apparent for the $Au/TiO_2/Al_2O_3$ (Fig. 10c, d) where the relative peak intensities of **1**, **2**, and **3** remained nearly unchanged.

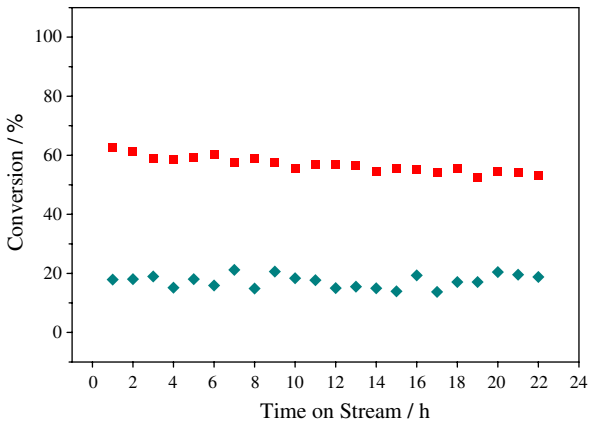

Fig. 8 Stability test in the presence of H_2. In this test, 37 mL/min 1% CO (balance air) and 5 mL/min pure H_2 continuously flowed thorough 10 mg $Au/TiO_2/\gamma\text{-}Al_2O_3$ at 23 °C. The CO conversion (■) and H_2 conversion (◆) were recorded. The $\gamma\text{-}Al_2O_3$ was from calcining AlOOH (Aldrich) in a muffle oven at 500 °C

4 Discussion

Because gold on TiO_2 is usually more active than gold on Al_2O_3 [6], the observed promotion of Au/Al_2O_3 by introducing a TiO_2 component is justified. However, that effect became obvious only when the Au/TiO_2/AlOOH and $Au/TiO_2/\gamma\text{-}Al_2O_3$ catalysts were pretreated at elevated temperatures before the reaction testing (Table 1). At least three possible reasons to account for such unexpected observation may be considered. The first possibility is that the TiO_2-modified surface may be affected by residual organic fragments. In our experiments, TiO_2 is grafted onto the AlOOH and $\gamma\text{-}Al_2O_3$ surfaces using $Ti(OC_4H_9)_4$ precursor. Although the anchored moieties were washed several times by water at ambient temperature, organic species may not be sufficiently hydrolyzed and removed [48], so the pretreatment of Au/TiO_2/AlOOH and $Au/TiO_2/\gamma\text{-}Al_2O_3$ catalysts in O_2–He at elevated temperatures might remove the residual organic fragments that had partially masked the inherent activity of these catalysts. However, this proposal cannot explain why as-synthesized Au/TiO_2/AlOOH and $Au/TiO_2/\gamma\text{-}Al_2O_3$ catalysts are still very active for CO oxidation at room temperature (Table 1).

A second possibility is that the presence of TiO_2 may stabilize surface Al–OH groups of Al_2O_3 upon thermal treatment, which are beneficial for CO oxidation [1–5]. This hypothesis is supported by the NMR results which show that the Al–OH component (signal **2**) is less affected by 500 °C-pretreatment on the TiO_2-modified catalyst. It is known that these hydroxyl groups play a beneficial role in the reaction mechanism in alumina-supported catalysts [13]. However, this hypothesis does not justify why 500 °C-pretreated $Au/TiO_2/\gamma\text{-}Al_2O_3$ is much more active than either as-synthesized $Au/\gamma\text{-}Al_2O_3$ or as-synthesized $Au/TiO_2/\gamma\text{-}Al_2O_3$ given that their relative peak intensities of **1**, **2**, and **3** are similar (Fig. 10).

For the third possibility, the support–metal interaction is optimized, and new Au–TiO_2 active sites are formed through thermal pretreatment. For instance, Haruta et al. mechanically mixed colloidal gold and TiO_2 powder, and found that high-temperature calcination made the catalyst

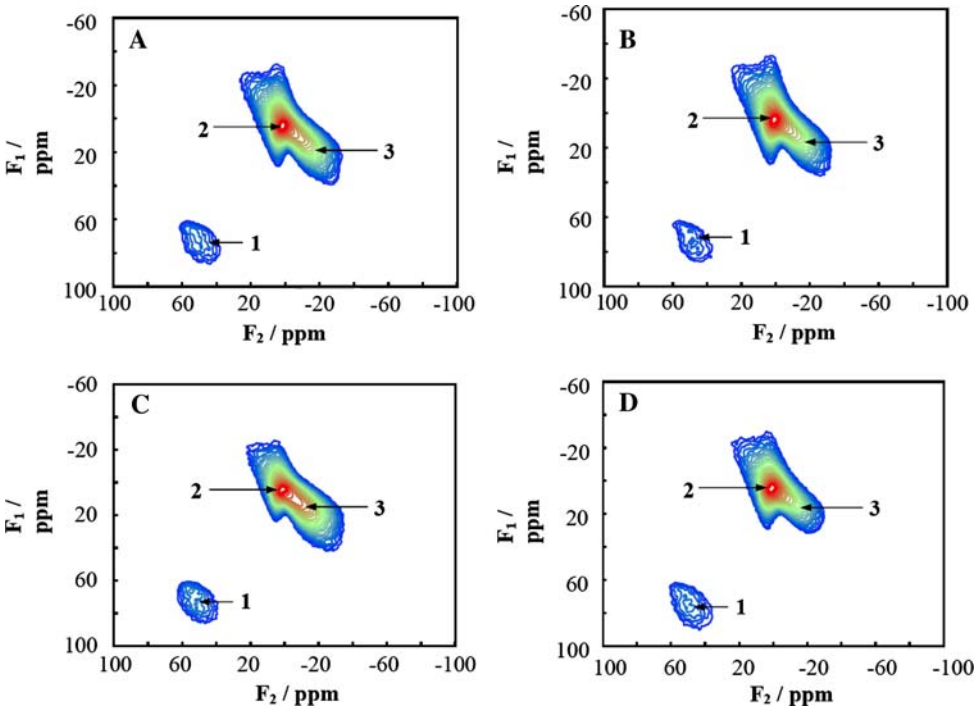

Fig. 9 ^{27}Al MQMAS NMR spectra of as-synthesized $Au/\gamma\text{-}Al_2O_3$ (**a**), 500 °C-pretreated $Au/\gamma\text{-}Al_2O_3$ (**b**), as-synthesized $Au/TiO_2/\gamma\text{-}Al_2O_3$ (C), and 500 °C-pretreated $Au/TiO_2/\gamma\text{-}Al_2O_3$ (**d**). F_2 and F_1 represent the MAS and isotropic projection. The $\gamma\text{-}Al_2O_3$ support was derived from calcining AlOOH (Aldrich) in a muffle oven at 500 °C

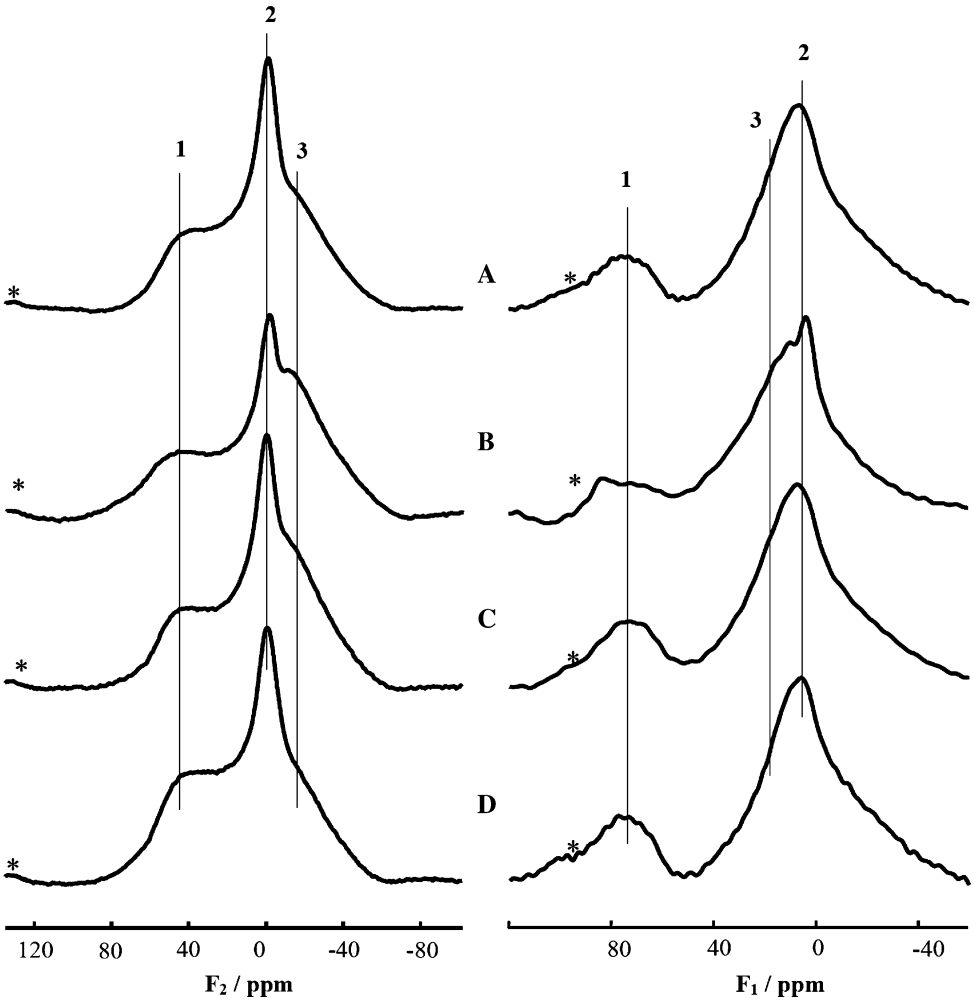

Fig. 10 Projections of ^{27}Al MQMAS NMR spectra of as-synthesized Au/γ-Al_2O_3 (**a**), 500 °C-pretreated Au/γ-Al_2O_3 (**b**), as-synthesized Au/TiO_2/γ-Al_2O_3 (**c**), and 500 °C-pretreated Au/TiO_2/γ-Al_2O_3 (**d**) along F_2 (left) and F_1 (right). Asterisks indicate spinning sidebands. The γ-Al_2O_3 support was derived from calcining AlOOH (Aldrich) in a muffle oven at 500 °C

more active. They proposed that a strong contact between gold particles and TiO_2 support was formed upon calcination [49]. In our current case, taking Au/TiO_2/γ-Al_2O_3 (γ-Al_2O_3 supports were prepared by calcining AlOOH-Aldrich and AlOOH-CATAPAL A in a muffle oven) as an example, the Ti loadings are 2.1 and 2.2 wt.% (Table 1), respectively. These Ti loading values correspond to 2.3 and 2.3 wt.% for gold-free TiO_2/γ-Al_2O_3. Assuming that each $Ti(OH)_4$ group condenses with one Al–OH group, and talking into account the surface areas of these TiO_2/γ-Al_2O_3 supports (180 and 230 m^2/g), the surface Al–O–$Ti(OH)_3$ densities are calculated to be 1.6 and 1.3/nm^2, respectively. That means only 40% and 33% Al–OH groups are used to form Al–O–$Ti(OH)_3$, assuming that the surface density of Al–OH on γ-Al_2O_3 is 4/nm^2 [50]. Because there are also Al–O–Al groups in addition to Al–OH groups on γ-Al_2O_3, the surface coverage of Ti species in our case is well below one monolayer. Therefore, there exist possibilities for gold nanoparticles to sit on top of TiO_2, Al_2O_3, and the interface between TiO_2 and Al_2O_3. For reference, the surface gold densities of these Au/TiO_2/γ-Al_2O_3 catalysts were estimated as 1.3 and 0.4 gold atom/nm^2, respectively.

The $Au(OH)_xCl_{4-x}^-$ solution was adjusted to pH 10 before deposition–precipitation. Considering that the isoelectric points of TiO_2 and Al_2O_3 are 5 and 9, respectively [4], the gold precursor may preferentially deposit onto Al_2O_3 sites because of closer charge match. Thus, the activity of as-synthesized Au/TiO_2/Al_2O_3 is similar to the corresponding as-synthesized Au/Al_2O_3 (Figs. 1, 3). Upon pretreatment at 500 °C, gold nanoclusters evolve into more observable gold nanoparticles (Figs. 2, 4). This thermal process may cause the migration of gold (Figs. 2, 4) and spontaneous dispersion of TiO_2 on the support [51], creating more Au–TiO_2 contacts. Since Au–TiO_2 interface is known to be more active than Au–Al_2O_3 interface for CO oxidation [1–5], the higher activity of Au/TiO_2/Al_2O_3 compared to Au/Al_2O_3 is justified. In the literature, the modification of SiO_2 support by TiO_2 coating can also make the resulting Au/TiO_2/SiO_2 catalysts more active for CO oxidation than Au/SiO_2 [25, 31, 36, 52]. For instance, Zhu et al. found that the T_{50} value of 500 °C-pretreated

Au/SiO_2 synthesized using $Au(en)_2Cl_3$ as the precursor was −8 °C, whereas that of 500 °C-pretreated $Au/TiO_2/SiO_2$ was −40 °C [31].

Since Au–TiO_2 interface is proposed for the enhanced catalytic activity of $Au/TiO_2/Al_2O_3$, then one may ask why 500 °C-pretreated $Au/TiO_2/Al_2O_3$ is much more active than 500 °C-pretreated Au/TiO_2 [10] although the latter also has Au–TiO_2 interface. The answer is that gold particle size on neat TiO_2 increase significantly to 5–30 nm upon such treatment [10], whereas gold particle size on TiO_2/Al_2O_3 remain to be small (Figs. 2, 4). Our 500 °C-pretreated $Au/TiO_2/Al_2O_3$ catalysts are even more active than 500 °C-pretreated $Au/Al_2O_3/TiO_2$ reported in our previous communication [10] because the activity of the latter is limited by the sintering problem associated with Au/TiO_2 and less active Au–Al_2O_3 interface. Namely, in our previous work [10], 500 °C-pretreated Au/TiO_2 itself exhibits a T_{50} value of 125 °C, so even if Al_2O_3 additive is used to promote the catalyst, the T_{50} of 500 °C-pretreated $Au/Al_2O_3/TiO_2$ is −17 °C, but not even lower. Nevertheless, in our current study, 500 °C-pretreated Au/Al_2O_3 shows better activity ($T_{50} = 17°$) due to less sintering (Figs. 1, 2), so the further presence of TiO_2 promoter makes the 500 °C-pretreated $Au/TiO_2/Al_2O_3$ even more active ($T_{50} = -48$ °C). Therefore, our current $Au/TiO_2/Al_2O_3$ design integrates both superior anti-thermal aging ability of Au/Al_2O_3 and active Au–TiO_2 interface. Further experiments such as XANES would be needed to systematically compare the local structures of $Au/TiO_2/Al_2O_3$ and $Au/Al_2O_3/TiO_2$.

5 Conclusions

The surfaces of various $Al_2O_3 \cdot xH_2O$ were modified with TiO_2 using a surface-sol–gel process, and gold nanoparticles were subsequently loaded via a deposition–precipitation method. Finely divided gold nanoparticles were present on the surface-modified supports even after high-temperature pretreatment. The TiO_2 additive played an important role in the enhancement of the activity of the calcined gold nanocatalysts, and the high-temperature pretreatment could make the TiO_2-promoted catalysts even more active for CO oxidation in certain cases. Support effects were also observed, because the catalysts made using amorphous $Al(OH)_3$ or highly crystalline γ-Al_2O_3 as the precursor were less active for CO oxidation. Detailed studies on the structural mechanism for the unusual activation are warranted, and extension of this surface-modification methodology to other systems is needed to invent new catalysts with enhanced catalytic performance.

Acknowledgments This work was supported by the Office of Basic Energy Sciences, U.S. Department of Energy. The Oak Ridge National Laboratory is managed by UT-Battelle, LLC for the U.S. DOE under Contract DE-AC05-00OR22725. This research was supported in part by the appointment for W. F. Yan, Z. Ma, S. M. Mahurin, and J. Jiao to the ORNL Research Associates Program, administered jointly by ORNL and the Oak Ridge Associated Universities.

References

1. Haruta M, Daté M (2001) Appl Catal A 222:427
2. Choudhary TV, Goodman DW (2002) Top Catal 21:25
3. Hashmi ASK, Hutchings GJ (2006) Angew Chem Int Ed 45:7896
4. Bond GC, Louis C, Thompson DT (2006) Catalysis by gold. Imperial College Press, London
5. Kung MC, Davis RJ, Kung HH (2007) J Phys Chem C 111:11767
6. Schubert MM, Hackenberg S, van Veen AC, Muhler M, Plzak V, Behm RJ (2001) J Catal 197:113
7. Wu S-H, Zheng X-C, Wang S-R, Han D-Z, Huang W-P, Zhang S-M (2004) Catal Lett 96:49
8. Yan WF, Chen B, Mahurin SM, Dai S, Overbury SH (2004) Chem Commun 1918
9. Yan WF, Chen B, Mahurin SM, Schwartz V, Mullins DR, Lupini AR, Pennycook SJ, Dai S, Overbury SH (2005) J Phys Chem B 109:10676
10. Yan WF, Mahurin SM, Pan ZW, Overbury SH, Dai S (2005) J Am Chem Soc 127:10480
11. Chen YJ, Yeh CT (2001) J Catal 200:59
12. Lee S-J, Gavriilidis A (2002) J Catal 206:305
13. Costello CK, Yang JH, Law HY, Wang Y, Lin JN, Marks LD, Kung MC, Kung HH (2003) Appl Catal A 243:15
14. Xu Q, Kharas KCC, Datye AK (2003) Catal Lett 85:229
15. Calla JT, Davis RJ (2005) Catal Lett 99:21
16. Veith GM, Lupini AR, Pennycook SJ, Ownby GW, Dudney NJ (2005) J Catal 231:151
17. Han Y-F, Zhong ZY, Ramesh K, Chen F, Chen L (2007) J Phys Chem C 111:3163
18. Zou X-H, Qi S-X, Suo Z-H, An L-D, Li F (2007) Catal Commun 8:784
19. Grisel RJH, Weststrate CJ, Goossens A, Crajé MWJ, van der Kraan AM, Nieuwenhuys BE (2002) Catal Today 72:123
20. Centeno MA, Paulis M, Montes M, Odriozola JA (2002) Appl Catal A 234:65
21. Wang DH, Hao ZP, Cheng DY, Shi XC, Hu C (2003) J Mol Catal A 200:229
22. Gluhoi AC, Bogdanchikova N, Nieuwenhuys BE (2005) J Catal 232:96
23. Centeno MA, Portales C, Carrizosa I, Odriozola JA (2005) Catal Lett 102:289
24. Gluhoi AC, Tang X, Marginean P, Nieuwenhuys BE (2006) Top Catal 39:101
25. Yan WF, Chen B, Mahurin SM, Hagaman EW, Dai S, Overbury SH (2004) J Phys Chem B 108:2793
26. Yan WF, Mahurin SM, Chen B, Overbury SH, Dai S (2005) J Phys Chem B 109:15489
27. Dai S, Yan WF (2006) Surface-stabilized gold nanocatalysts. US Patent Application Publication, 2006/0293175 A1
28. Ma Z, Brown S, Overbury SH, Dai S (2007) Appl Catal A 327:226
29. Ma Z, Overbury SH, Dai S (2007) J Mol Catal A 273:186
30. Ma Z, Liang CD, Overbury SH, Dai S (2007) J Catal 252:119
31. Zhu HG, Ma Z, Clark JC, Pan ZW, Overbury SH, Dai S (2007) Appl Catal A 326:89
32. Zhu HG, Ma Z, Overbury SH, Dai S (2007) Catal Lett 116:128
33. Yonezawa T, Matsune H, Kunitake T (1999) Chem Mater 11:33

34. Amoureux J-P, Fernandez C, Steuernagel S (1996) J Magn Reson A 123:116
35. Rocha J, Morais CM, Fernandez C (2004) Top Curr Chem 246:141
36. Venezia AM, Liotta FL, Pantaleo G, Beck A, Horvath A, Geszti O, Kocsonya A, Guczi L (2006) Appl Catal A 310:114
37. Bandyopadhyay M, Korsak O, van den Berg MWE, Grunert W, Birkner A, Li W, Schüth F, Gies H (2006) Microporous Mesoporous Mater 89:158
38. Cozzolino M, Di Serio M, Tesser R, Santacesaria E (2007) Appl Catal A 325:256
39. Xu L-X, He C-H, Zhu M-Q, Wu K-J, Lai Y-L (2007) Catal Lett 118:248
40. Bond GC, Thompson DT (2000) Gold Bull 33:41
41. Corti CW, Holliday RJ, Thompson DT (2007) Top Catal 44:331
42. Deng XY, Ma Z, Yue YH, Gao Z (2001) J Catal 204:200
43. Manzoli M, Chiorino A, Boccuzzi F (2004) Appl Catal B 52:259
44. Azar M, Caps V, Morfin F, Rousset JL, Piednoir A, Bertolini JC, Piccolo L (2006) J Catal 239:307
45. Kraus H, Prins R, Kentgens APM (1996) J Phys Chem 100:16336
46. Jiao J, Kanellopoulos J, Wang W, Ray SS, Foerster H, Freude D, Hunger M (2005) Phys Chem Chem Phys 7:3221
47. Kanehashi K, Saito K (2004) Fuel Process Technol 85:873
48. Pârvulescu VI, Marcu V (2006) In: Richards R (ed) Surface and nanomolecular catalysis. Taylor & Francis (CRC Press), Boca Raton, p 427
49. Tsubota S, Nakamura T, Tanaka K, Haruta M (1998) Catal Lett 56:131
50. Joubert J, Dellbecq F, Sautet P (2007) J Catal 507
51. Xie YC, Tang YQ (1990) Adv Catal 37:1
52. Tai Y, Murakami J, Tajiri K, Ohashi F, Daté M, Tsubota S (2004) Appl Catal A 268:183